

Large Variety of New Pulsating Stars in the OGLE-III Galactic Disk Fields*

P. Pietrukowicz¹, W. A. Dziembowski¹, P. Mróz¹,
I. Soszyński¹, A. Udalski¹, R. Poleski^{1,2},
M. K. Szymański¹, M. Kubiak¹, G. Pietrzyński^{1,3},
Ł. Wyrzykowski^{1,4}, K. Ulaczyk¹,
S. Kozłowski¹ and J. Skowron¹

¹Warsaw University Observatory, Al. Ujazdowskie 4, 00-478 Warszawa, Poland
e-mail: (pietruk,wd,pmroz,soszynski,udalski,rpoleski,msz,mk,pietrzyn,
wyrzykow,kulaczyk,simkoz,jskowron)@astrouw.edu.pl

² Department of Astronomy, Ohio State University, 140 W. 18th Ave.,
Columbus, OH 43210, USA

³ Universidad de Concepción, Departamento de Astronomía,
Casilla 160-C, Concepción, Chile

⁴ Institute of Astronomy, University of Cambridge, Madingley Road,
Cambridge CB3 0HA, UK

ABSTRACT

We present the results of a search for pulsating stars in the 7.12 deg² OGLE-III Galactic disk area in the direction tangent to the Centaurus Arm. We report the identification of 20 Classical Cepheids, 45 RR Lyr type stars, 31 Long-Period Variables, such as Miras and Semi-Regular Variables, one pulsating white dwarf, and 58 very likely δ Sct type stars. Based on asteroseismic models constructed for one quadruple-mode and six triple-mode δ Sct type pulsators, we estimated masses, metallicities, ages, and distance moduli to these objects. The modeled stars have masses in the range 0.9–2.5 M_{\odot} and are located at distances between 2.5 kpc and 6.2 kpc. Two triple-mode and one double-mode pulsators seem to be Population II stars of the SX Phe type, probably from the Galactic halo. Our sample also includes candidates for Type II Cepheids and unclassified short-period ($P < 0.23$ d) multi-mode stars which could be either δ Sct or β Cep type stars. One of the detected variables is a very likely δ Sct star with an exceptionally high peak-to-peak I -band amplitude of 0.35 mag at the very short period of 0.0196 d. All reported pulsating variables but one object are new discoveries. They are included in the OGLE-III Catalog of Variable Stars.

Finally, we introduce the on-going OGLE-IV Galactic Disk Survey, which covers more than half of the Galactic plane. For the purposes of future works on the spiral structure and star formation history of the Milky Way, we have already compiled a list of known Galactic Classical Cepheids.

Galaxy: disk – Stars: variables: Cepheids – Stars: variables: delta Scuti –
Stars: variables: RR Lyrae – variables: general

1 Introduction

Pulsations are present in many phases of stellar evolution and are reflected in a variety of observed types of pulsating variable stars. Pulsating stars occupy different regions on the Hertzsprung–Russell diagram. They are seen among main-sequence (MS) and post-MS stars (*e.g.*, β Cep, γ Dor, δ Sct type), giants (*e.g.*, Classical Cepheids, Miras, RR Lyr type), and white dwarfs (*e.g.*, ZZ Cet, V777 Her type).

Pulsations provide information on the structure and evolution of stars. The observed properties of Classical Cepheids (δ Cep type stars), such as periods,

*Based on observations obtained with the 1.3-m Warsaw telescope at the Las Campanas Observatory of the Carnegie Institution for Science.

amplitudes, and colors allow for testing of hydrodynamical models of stars (*e.g.*, Kanbur, Ngeow and Buchler 2004, Kanbur *et al.* 2010). Period changes in Classical Cepheids help to verify their evolutionary models (*e.g.*, Pietrukowicz 2003, Turner, Abdel-Sabour Abdel-Latif and Berdnikov 2006, Poleski 2008). Recent studies of period changes show that some Cepheids, including the nearest Polaris, are very likely undergoing enhanced mass loss (Neilson *et al.* 2012).

Better understanding of Cepheid structure provides greater insight into their use as standard candles. They serve as distance indicators to various regions of the Milky Way and to other galaxies in the Local Group and beyond. Classical Cepheids, as young and luminous stars, help to explore the distribution of elements in the Galactic disk (Luck *et al.* 2011) and trace its spiral structure (*e.g.*, Popova 2006, Majaess, Turner and Lane 2009, Bobylev and Bajkova 2012). Recent works indicate a steady decrease in metallicity in Cepheids with the increasing distance from the Galactic center in the thin disk and no correlation between the metallicity and the vertical distance from the Galactic plane (Genovali *et al.* 2013, Lemasle *et al.* 2013).

Numerous Classical Cepheids detected in the Large Magellanic Cloud (*e.g.*, Soszyński *et al.* 2008) were used for calibration of the extra-galactic distance scale (*e.g.*, Storm *et al.* 2011). The Cepheid period-luminosity relation allows for the determination of the distance to many nearby galaxies, such as M31 (*e.g.*, Vilardell, Jordi and Ribas 2007, Riess, Fliri and Valls-Gabaud 2012), M33 (*e.g.*, Gieren *et al.* 2013), NGC 300 (*e.g.*, Gieren *et al.* 2004), IC 1613 (*e.g.*, Tammann, Reindl and Sandage 2011), and more distant, like M81 (Freedman *et al.* 1994).

RR Lyr type stars are tracers of old populations. So far, thousands of such stars have been discovered in the Galactic bulge (*e.g.*, Soszyński *et al.* 2011a), halo (*e.g.*, Szczygieł, Pojmański and Pilecki 2009, Sesar *et al.* 2010, Akhter *et al.* 2012, Süveges *et al.* 2012), and thick disk (*e.g.*, Kinemuchi *et al.* 2006, Bernhard and Wils 2009, Mateu *et al.* 2012). Observations of Galactic halo variables show the presence of two groups having different metal content and indicating that the halo was formed by at least two distinct accretion processes (Miceli *et al.* 2008). One of unsolved issues is whether the bulge and metal-rich halo RR Lyr stars constitute the same population (Pietrukowicz *et al.* 2012). RR Lyr variables serve as distance indicators and probes of formation history in nearby galaxies (*e.g.*, Pietrzyński *et al.* 2008, Greco *et al.* 2009, Sarajedini *et al.* 2009, Yang *et al.* 2010).

Another class of pulsating giants, Mira stars, are also used for measuring distances within the local universe (*e.g.*, Whitelock *et al.* 2009, Menzies *et al.* 2010). These bright high-amplitude Long-Period Variable (LPV) stars are seen from a distance of several Mpc from the Sun (*e.g.*, in Cen A, Rejkuba 2004).

Pulsating variables of δ Sct, γ Dor, β Cep type, and Slowly Pulsating B (SPB) stars showing multiple modes are of particular interest for testing seismic models of MS and post-MS stars (*e.g.*, Daszyńska-Daszkiewicz, Dziembowski and Pamyatnykh 2005, Balona and Dziembowski 2011, Balona *et al.* 2012). Information on periodicities permit the determination of basic parameters of stars, such as mass, effective temperature, and metallicity (*e.g.*, Li, Xu and Li 2010, Breger *et al.* 2011, Paparó *et al.* 2013). Recently, Suárez *et al.* (2010) proposed to use rotational splitting asymmetries to probe the internal rotation profile of β Cep type stars.

For more than two decades the number of detected pulsating stars has increased rapidly. For example, the Optical Gravitational Lensing Experiment (OGLE) – a long-term large-scale sky survey focused on stellar variability (Udal-

ski *et al.* 1992, Udalski 2003) has already discovered and classified about 400 000 pulsating variables in the Galactic bulge and Magellanic Clouds (*e.g.*, Soszyński *et al.* 2010, 2011ab, 2013).

This paper presents results of a search for pulsating stars in twenty-one OGLE-III fields located in the Galactic disk toward constellations of Carina, Centaurus, and Musca. In the following sections we describe: the observations and data reductions (Section 2), the on-line material (Section 3), the detected variable stars of different types in details (Sections 4), and the completeness of the search (Section 5). In Section 6, we summarize our results, while in the last section, Section 7, we introduce the on-going OGLE-IV Galactic Disk Survey.

2 Observations and Data Reductions

The observations presented in this paper were collected with the 1.3-m Warsaw telescope at Las Campanas Observatory, Chile, during the third phase of the Optical Gravitational Lensing Experiment (OGLE-III) in years 2001–2009. The observatory is operated by the Carnegie Institution for Science. The OGLE-III CCD camera consisted of eight chips with the total field of view of $35' \times 35'$ and the scale of 0.26 arcsec/pixel. More details on the instrumentation setup can be found in Udalski (2003).

The OGLE-III Galactic disk fields covered an area of 7.12 deg^2 near the Galactic plane between longitudes $+288^\circ$ and $+308^\circ$. Coordinates of the centers, the time coverage, and the number of data points of the monitored fields are given in Table 1 and shown in Figs. 1–2 in Pietrukowicz *et al.* (2013). A significant majority of frames (815–2698 per field) were collected in the standard *I*-band filter with an exposure time of 120 or 180 s. Additional observations, consisting of only 3–8 measurements, were taken in the *V*-band filter with an exposure time of 240 s. A total number of approximately 8.8×10^6 stars with brightness between $I = 12.5 \text{ mag}$ and $I = 21.5 \text{ mag}$ was observed (Szymański *et al.* 2010).

The photometry was obtained with the standard OGLE data reduction pipeline (Udalski *et al.* 2008) using the Difference Image Analysis (Alard and Lupton 1998, Woźniak 2000). We performed a frequency search up to 24 d^{-1} with the help of the FNPEAKS code (written by Z. Kołaczowski, private communication) for stars containing at least 30 measurements in the *I*-band. Around 345 500 detections were visually inspected for any kind of variability. This was done in two stages. In the first stage, we inspected about 100 500 stars having a variability signal-to-noise ratio $S/N \geq 14$, and in the second stage about 245 000 objects with $10 \leq S/N < 14$. We also performed an additional search for high frequencies between 24 d^{-1} and 100 d^{-1} for stars with $I < 18.5 \text{ mag}$ and $V - I < 0.7 \text{ mag}$. Our searches resulted in thousands of miscellaneous variables (*e.g.*, Mróz *et al.* 2013, Pietrukowicz *et al.* 2013, 2014, in preparation).

Based on the initially determined period and shape of the light curve we classified our candidate pulsating stars into the following types: Classical Cepheids (20 objects), RR Lyr type stars (45 objects), Long-Period Variables (31 objects), and short-period stars for further analysis (about 2000 objects with $P < 0.25 \text{ d}$). We manually removed obvious outliers from the light curves of our stars and improved their periods using the TATRY code (Schwarzenberg-Czerny 1996). In the next step, we searched the Cepheids and short-period stars for additional modes. Based on the periods, period ratios, and amplitudes of the short-period variables we selected 57 good candidates for $\delta \text{ Sct}$ type stars. Another candidate

for a δ Sct variable together with a very likely pulsating white dwarf were found as a result of the high-frequency search.

Each variable was calibrated from the instrumental to the standard magnitudes using transformation relations given in Udalski *et al.* (2008). Since the number of V -band measurements is very small, we rely on average instrumental brightnesses $\langle v \rangle$ and $\langle i \rangle$, and color $\langle v \rangle - \langle i \rangle$. For high-amplitude stars, we fit the instrumental i -band light curve to the instrumental v -band data by adjusting the amplitude and phase shift. The average brightness in both passbands was derived from the fits. In the case of low-amplitude multi-mode pulsating stars the $\langle v \rangle$ and $\langle i \rangle$ values were determined as the arithmetic mean from all measurements after converting magnitudes into fluxes. For stars without any available V -band measurement, except LPVs, we assumed an average $V - I$ color of neighboring stars within a radius of $1'0$ taken from the photometric maps in Szymański *et al.* (2010). For LPVs without points in V , we assumed an average $V - I$ color determined from the remaining LPVs. For all stars with $V - I > 1.5$ mag the final I -band photometry had to be additionally corrected according to formula presented in Szymański *et al.* (2011).

3 On-line Data

The catalog of pulsating stars in the Galactic disk fields, containing tables with basic parameters, time-series I - and V -band photometry, and finding charts, is available to the astronomical community from the OGLE Internet Archive:

<http://ogle.astroww.edu.pl>

and

<ftp://ftp.astroww.edu.pl/ogle/ogle3/OIII-CVS/gd/>

where one can find the following catalogs on pulsating stars: `cep`, `dsct`, `lpv`, `rrlyr`, `t2cep`, `wd`, and `unclassified`. The stars are arranged according to increasing right ascension and named as OGLE-GD-CEP-NNNN, OGLE-GD-DSCT-NNNN, OGLE-GD-LPV-NNNN, OGLE-GD-RRLYR-NNNN, OGLE-GD-T2CEP-NNNN, and OGLE-GD-WD-NNNN, where NNNN are four-digit consecutive numbers for each of the type. In the case of short-period unclassified variables we leave the name as the following catenation: FIELD.CHIP.ID. In the data tables, we provide coordinates of the variables, their pulsation periods, period uncertainties, information on brightness, and classification to a subtype, if exists.

4 Detected Pulsating Variables

4.1 Classical Cepheids

Our search for variable objects brings identification of 20 Classical Cepheids. All Cepheids but one object are new discoveries. Variable OGLE-GD-CEP-0019 was detected by the EROS-II collaboration during the Galactic Spiral Arms (GSA) observation program and named EROS2 GSA J133319-640707 (Derue *et al.* 2002). Light curves of all OGLE-III disk Classical Cepheids are presented in Fig. 1. Eight stars are double-mode pulsators (beat Cepheids) of which three pulsate in the fundamental mode (F) and first overtone (1O), four in the first and second overtone (2O), and one object, OGLE-GD-CEP-0001, in the first

overtone and a second mode of unknown origin (labeled with X). Ten Cepheids pulsate in the fundamental mode. The pulsation period of OGLE-GD-CEP-0010 is longer than 10 d, hence this star is younger than 50 Myr (based on models in Bono *et al.* 2005). From the information on the period ratio for F/10 pulsators, we infer that OGLE-GD-CEP-0012 and OGLE-GD-CEP-0016 are very likely objects of lower metallicity in comparison to other stars of this type (see Fig. 10 and discussion in Section 4.5).

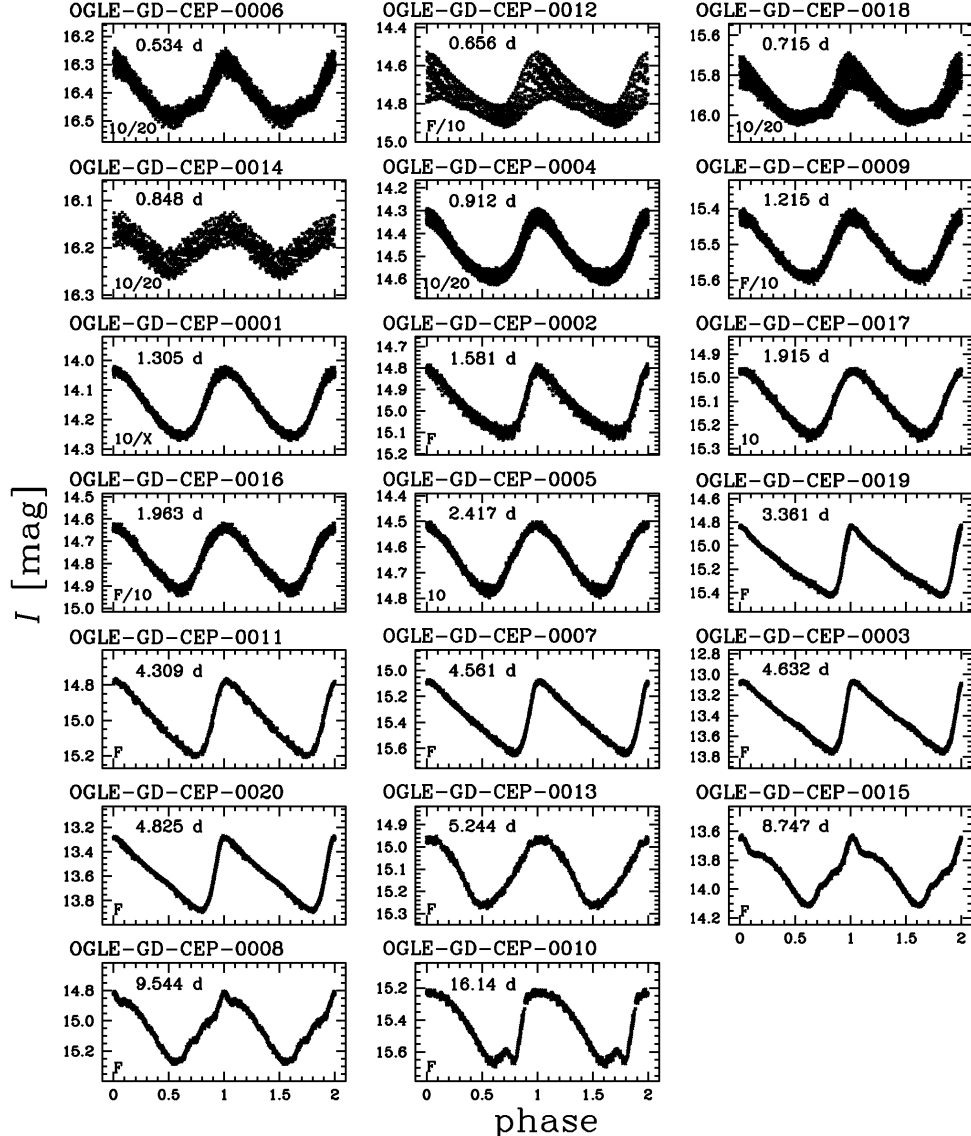


Fig. 1. Phased light curves of 20 Classical Cepheids detected in the OGLE-III disk area. Objects are sorted according to increasing period.

All Cepheids have the average apparent brightness between $I = 13.4$ mag and $I = 16.4$ mag. Star OGLE-GD-CEP-0011 has no measurement in V due to unfortunate position just outside the reference image in this band. The observed $V - I$ color of the remaining 19 Classical Cepheids is in a range between 1.1 mag and 4.2 mag. Such a wide magnitude range is the result of the non-uniformly distributed interstellar extinction in the Galactic disk. It is worth to note that

the monitored area contains other eleven known Classical Cepheids, but all of them are saturated in the OGLE data.

4.2 Candidates for Type II Cepheids

The observed amplitudes (0.2–0.4 mag) and shape of the light curves of six stars (Fig. 2) resemble those of Type II Cepheids (*e.g.*, Soszynski *et al.* 2011b). Five stars with periods between 5 d and 20 d could be of W Vir type, while the 35.15 d star OGLE-GD-T2CEP-0004 is a probable RV Tau type variable. For object OGLE-GD-T2CEP-0001 there is no color information due to heavy reddening, while the remaining stars have $V-I$ between 1.9 and 2.7 mag. Their location in the I vs. $V-I$ diagrams (Fig. 3) is in agreement with the proposed types of old population Cepheids. However, our confidence is not full due to the fact that all objects but OGLE-GD-T2CEP-0001 were detected at an angular distance $< 0.8^\circ$ from the Galactic plane in fields observed for about one season only.

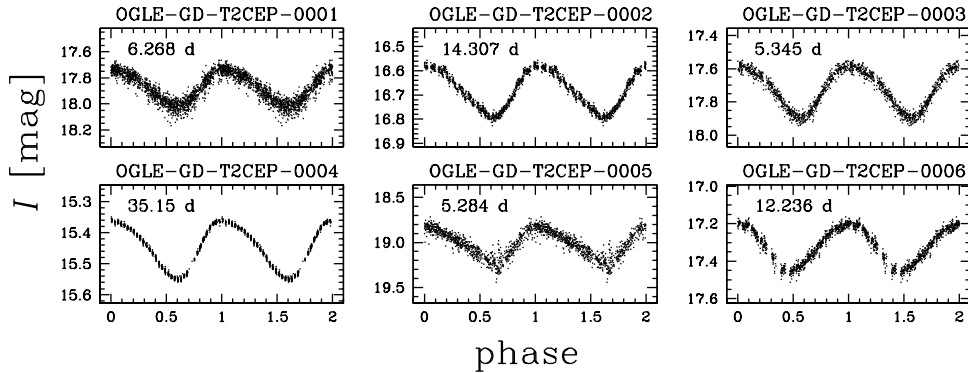


Fig. 2. Phased light curves of six candidates for Type II Cepheids.

4.3 RR Lyr type Stars

Within the twenty-one disk fields we found 45 RR Lyr stars of which 36 are of the type “ab” (fundamental mode) and nine of the type “c” (first overtone). Light curves of the variables are presented in Fig. 4. Object OGLE-GD-RRLYR-0005 was detected independently in two overlapping fields CAR109 and CAR115. The increased time span allowed a better determination of the pulsation period for this star. Twelve of our RRab variables (*i.e.*, one-third of the sample) exhibit the Blazhko effect (Blazhko 1907), which manifests as long-period modulations in the light curve shape (Smith 2004). The observed Blazhko periods are between 21 d and 90 d.

We used an empirical relation presented in Smolec (2005) to assess the metallicity of the RRab stars on the Jurcsik (1995) scale (J95):

$$[\text{Fe}/\text{H}]_{\text{J95}} = -3.142 - 4.902P + 0.824\phi_{31}, \quad \sigma_{\text{sys}} = 0.18,$$

where P is the pulsation period and $\phi_{31} = \phi_3 - 3\phi_1$ is a Fourier phase combination derived from the I -band light curve. In Fig. 5, we present the obtained metallicity distributions for all RRab stars as well as those without the Blazhko effect. The stars form essentially two groups: a metal-rich one with $[\text{Fe}/\text{H}]_{\text{J95}} \gtrsim -0.8$ and a metal-poor one with $[\text{Fe}/\text{H}]_{\text{J95}} \lesssim -0.8$. This division likely reflects the

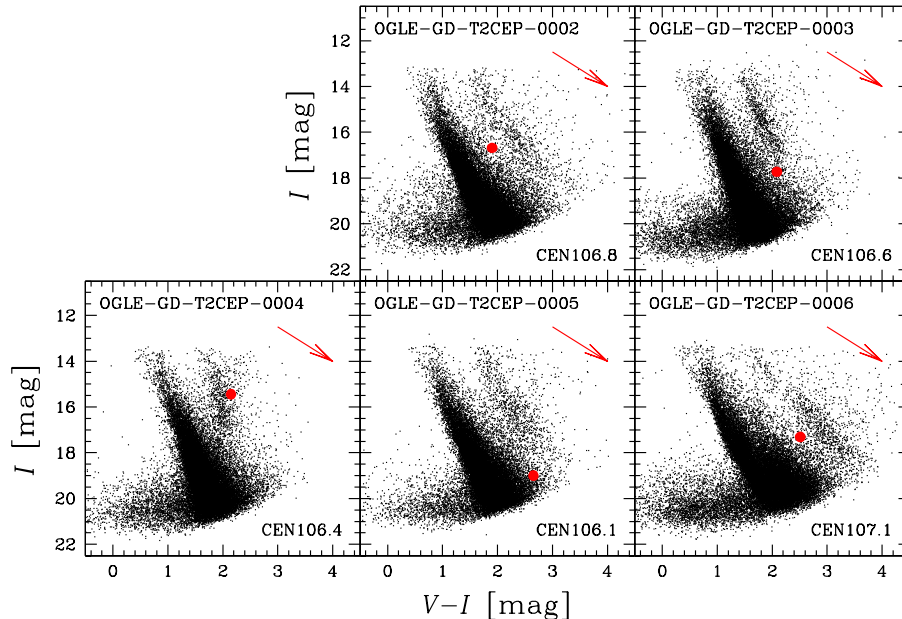


Fig. 3. Color-magnitude diagrams with marked positions (red points) of candidates for Type II Cepheids. Field name is given in each panel. Red arrows indicate the direction of reddening with an assumed ratio of total-to-selective extinction $R_I = A_I/E(V-I) = 1.5$.

presence of stars from two Galactic populations: the thick disk and halo, respectively. Such explanation is in agreement with properties of RR Lyr stars observed in the Galaxy (*e.g.*, Kinemuchi *et al.* 2006, Kinman, Morrison and Brown 2009, Szczygiel *et al.* 2009).

4.4 Long-Period Variables

We identified 31 new LPVs in the OGLE-III Galactic disk area. In Fig. 6, we present their I -band light curves phased with our best-measured pulsation periods. Eighteen of the LPVs are Mira stars, while the other thirteen objects are Semi-Regular Variable (SRV) stars. For ten LPVs the observations are insufficient to estimate their peak to peak amplitudes in I . Due to the lack of V -band data we were not able to assess the $V-I$ color for four Mira stars. Miras OGLE-GD-LPV-0023 and 0027 have the largest mean observed color among all detected variables within the OGLE-III disk fields, $V-I \approx 7.6$ mag.

4.5 δ Sct type Stars

We classified 58 stars as very likely δ Sct type variables. Fifty-seven of them were found during the search for frequencies lower than 24 d^{-1} and one object during the high-frequency search ($24\text{--}100 \text{ d}^{-1}$). The alternative within the realm of short-period pulsating stars is the β Cep type. The period ranges for these two types largely overlap, although β Cep stars have much higher masses and effective temperatures. Unfortunately, our data do not allow us to assess these parameters, mostly because of the heavy and unknown reddening in the observed regions. Thus, we cannot exclude that some of the stars, which we

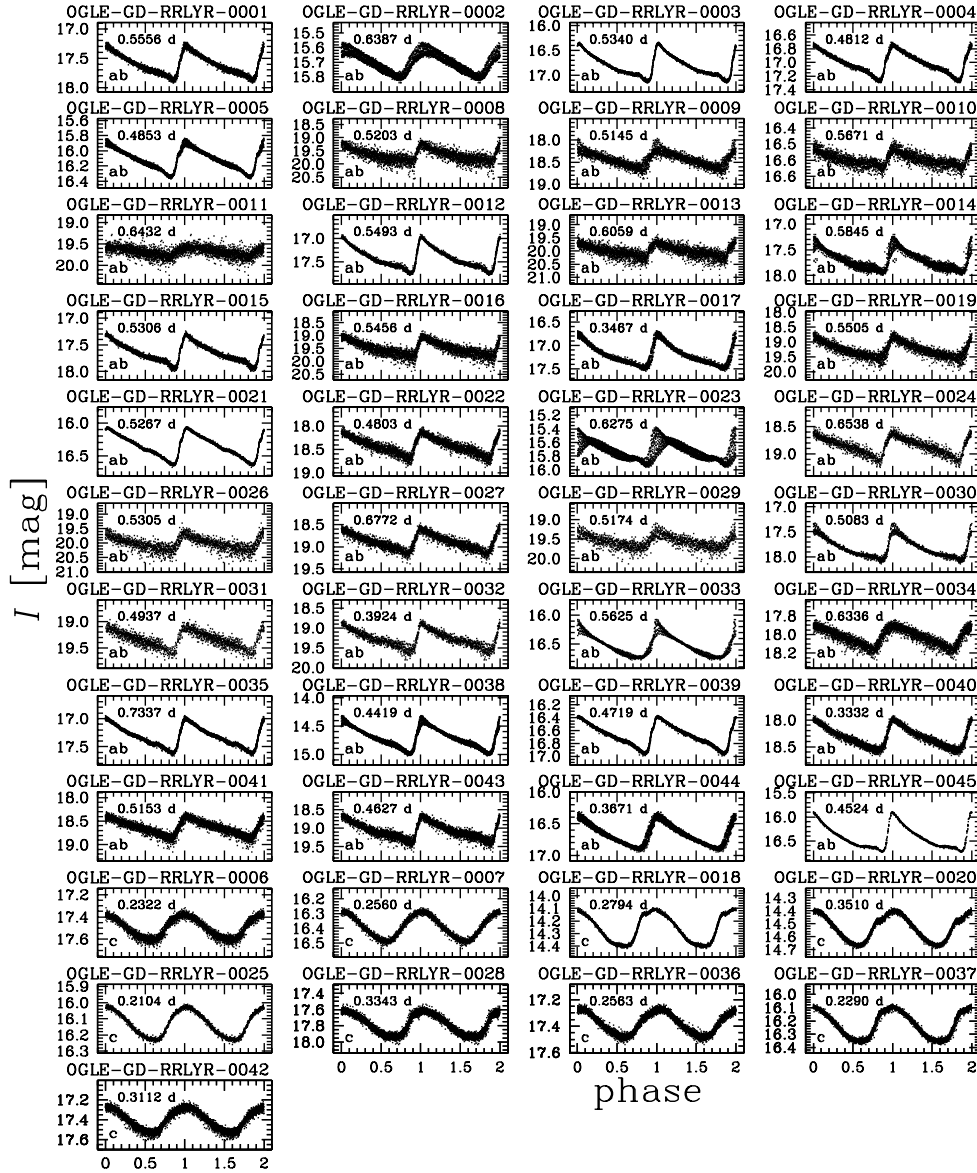


Fig. 4. Phased light curves of 45 RR Lyr variables found within the OGLE-III Galactic disk fields. The type of the variables is given in the lower left corner of each panel.

classified as δ Sct, may be in fact β Cep stars. However, this seems unlikely because amplitudes as high as in our stars (>0.1 mag) are rare in β Cep stars (see Stankov & Handler 2005). Furthermore, the period range in our multi-periodic objects is wider than typically found in β Cep stars.

Twenty-eight stars in our sample are fundamental-mode pulsators (see light curves in Fig. 7). Of course we cannot exclude that some other modes are excited in these objects, but their amplitudes must be much smaller. Stars with one or two dominant radial modes are known as High Amplitude Delta Scuti stars (HADS). They are rare. According to Lee *et al.* (2008) only about 0.3% of the total population of Galactic δ Sct stars belongs to this subtype. What causes that a star chooses this high-amplitude form of pulsation is unknown.

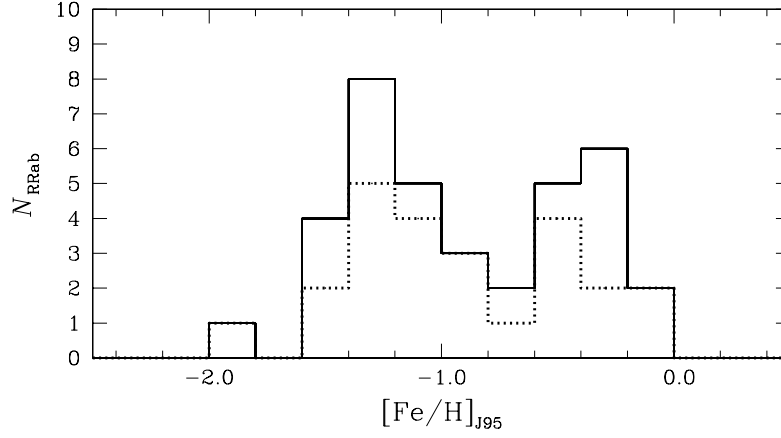


Fig. 5. Distributions of photometrically derived metallicities for all 36 newly detected RRab type stars (solid line) and a subgroup of 24 variables without the Blazhko effect (dotted line). The metallicity is given in the Jurcsik (1995) scale.

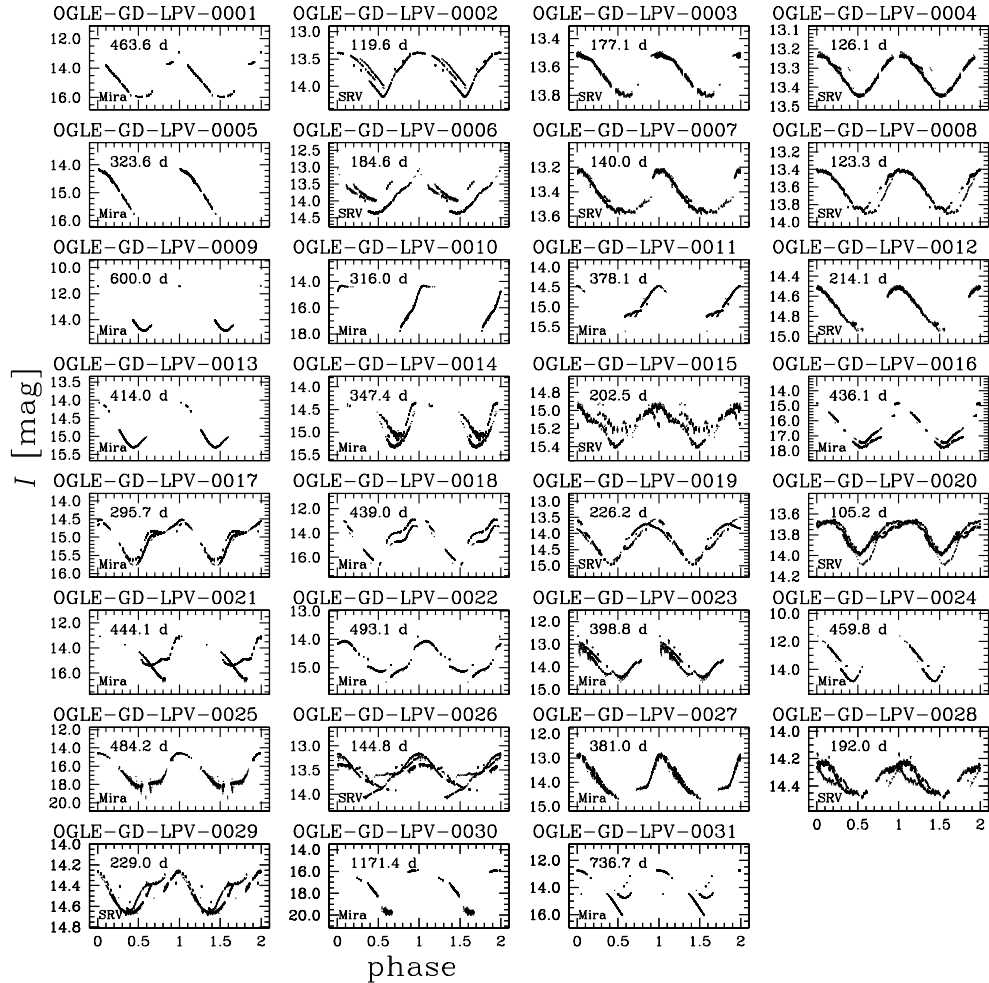


Fig. 6. Light curves of 31 LPVs detected in the OGLE-III disk area.

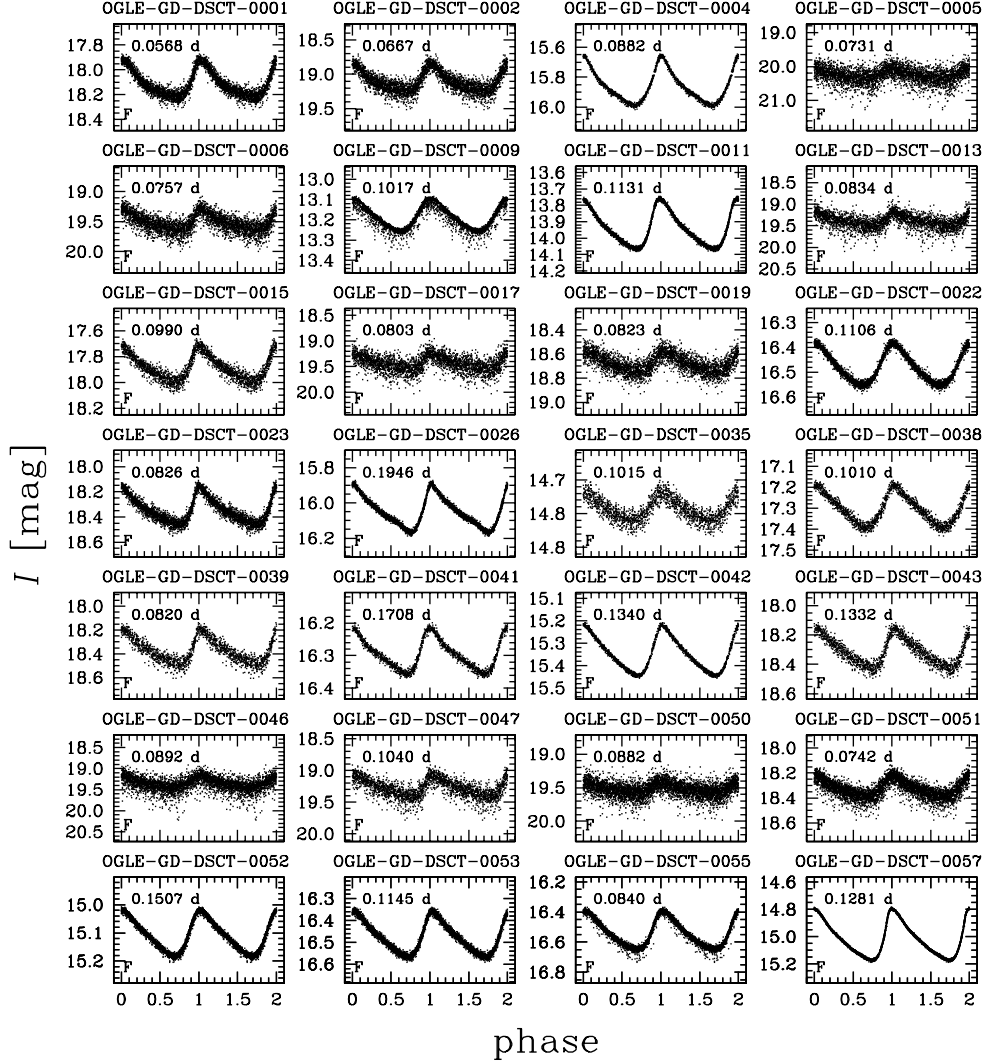


Fig. 7. Phased light curves of 28 detected fundamental-mode δ Sct type variables.

In the remaining 30 stars of our sample we detected at least two modes. Their light curves phased with the strongest period are plotted in Fig. 8. The amplitudes of light variations are large by δ Sct star standards. However, it is not clear if the dominant peaks are due to radial modes. In this work, we assume this to be the case. Only with this optimistic assumption an inference on stellar parameters based on periods alone is possible.

Twenty-two δ Sct stars exhibit two radial modes (in eighteen cases F and 1O), six stars exhibit three radial modes (mostly F, 1O, and 2O), and one star, OGLE-GD-DSCT-0025, seems to have four radial modes (F, 1O, 2O, and 3O, see periodograms in Fig. 9). In some of the stars, we detected additional non-radial modes. Objects with more than two *bona fide* radial modes are particularly valuable in this context. Table 1 lists data for such objects.

The identification of the radial orders of excited modes in multi-mode pulsators was done with the help of the Petersen diagram (shorter-to-longer period ratio *vs.* the logarithm of the longer period). The diagram, presented in Fig. 10,

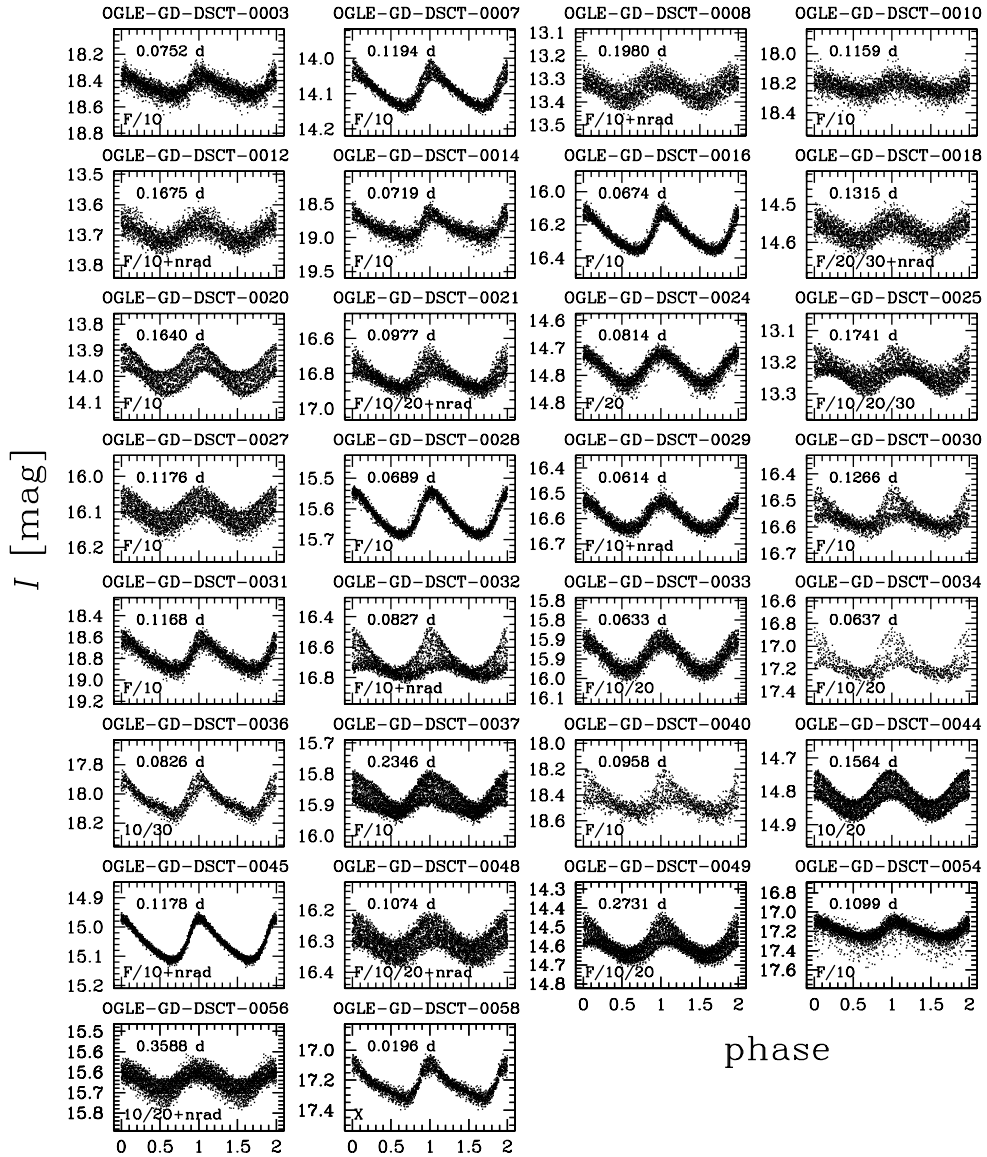


Fig. 8. Light curves of 30 detected multi-mode δ Sct type stars.

includes the multi-mode δ Sct as well as double-mode δ Cep type stars. The relations for the former type looks like continuations of the relations for multi-mode Cepheids. This has been already noted for numerous variables detected in the Large Magellanic Cloud (see Fig. 3 in Poleski *et al.* 2010) and is not surprising because post-MS δ Sct stars are just a low-mass version Cepheids crossing the instability strip for the first time. What matters is that this continuity supports the radial mode hypothesis for modes in δ Sct stars.

One of the disk Classical Cepheids, OGLE-GD-CEP-0001, is a first-overtone pulsator with an additional secondary period near $0.6P_{10}$. About 140 such Cepheids from the Small Magellanic Cloud (SMC) and 30 from the Large Magellanic Cloud (LMC) were reported in Soszyński *et al.* (2008) and Soszyński *et al.* (2010), respectively. The origin of this secondary period remains unknown.

An interesting application of the Petersen diagrams is probing of metal abun-

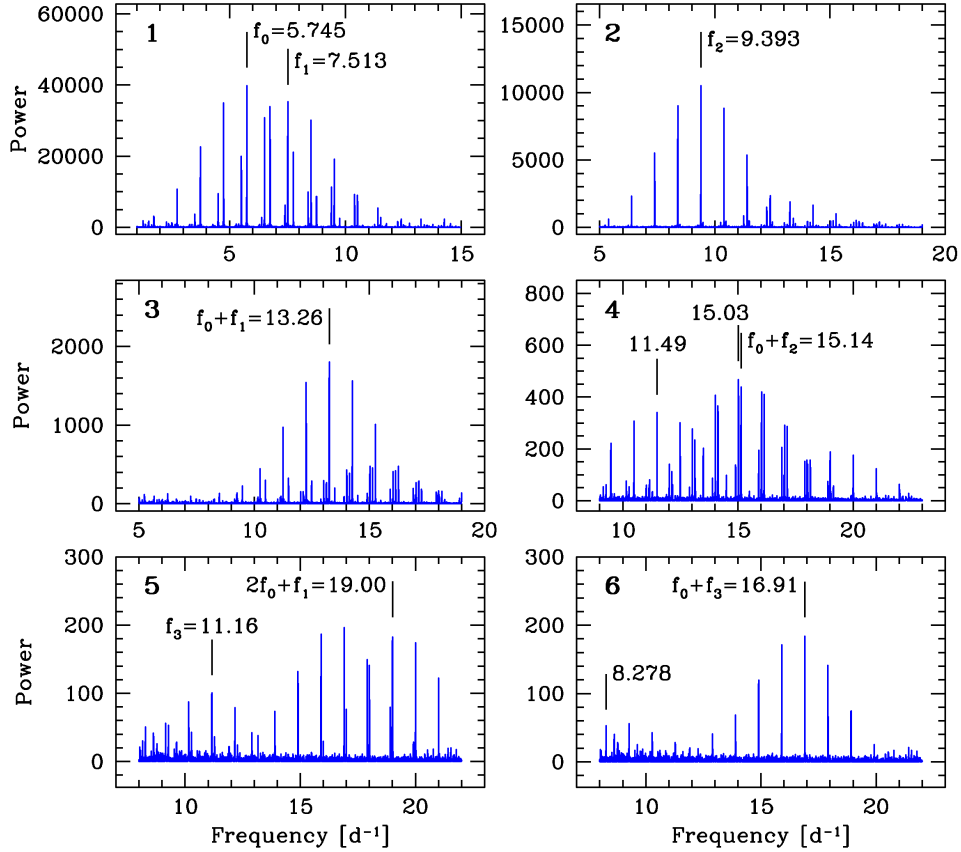


Fig. 9. Periodograms with marked frequencies after subsequent pre-whitenings (numbered in the upper left corners) for the quadruple-mode star OGLE-GD-DSCT-0025. Radial modes and their combinations are labeled.

Table 1: Observed periods for seven δ Sct type stars with at least three radial modes

Variable	P_F	P_{1O}	P_{2O}	P_{3O}
OGLE-GD-				
-DSCT-	[d]	[d]	[d]	[d]
-0018	0.13152629(81)	-	0.08140070(20)	0.06896097(53)
-0021	0.09766834(39)	0.07692128(44)	0.06186007(56)	-
-0025	0.1740594(19)	0.13310790(70)	0.10646403(51)	0.0896032(29)
-0033	0.06330743(12)	0.04894428(14)	0.03949024(70)	-
-0034	0.06369610(25)	0.04993199(9)	0.04106100(26)	-
-0048	0.10740182(5)	0.08293446(1)	0.06655117(3)	-
-0049	0.36141456(19)	0.27314926(19)	0.21699323(26)	-

dance in stars (see Popielski, Dziembowski and Cassisi 2000, Buchler and Szabó 2007, Buchler 2008, and Soszyński *et al.* 2011a for application to RR Lyr stars and Cepheids). We applied this tool to 27 δ Sct stars of our sample, which reveal pairs of radial modes of consecutive orders. The data are compared with model

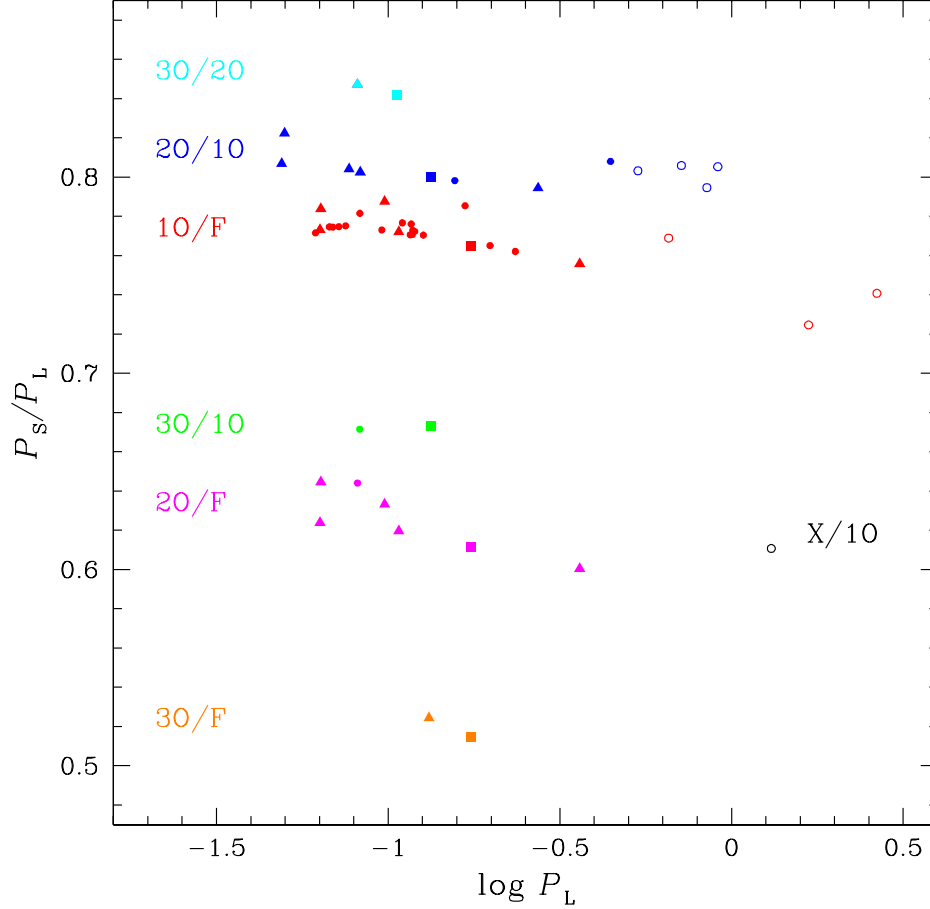


Fig. 10. Petersen diagram for multi-mode pulsators in the OGLE-III disk area. Open symbols correspond to Classical Cepheids, filled symbols to δ Sct type stars. Circles refer to double-mode, triangles – triple-mode, and squares – quadruple-mode pulsators.

values in the separate diagrams employing the (F,10) and (10,20) pairs shown in Fig. 11. The lines present the values calculated for stellar models along evolutionary tracks at selected metallicity parameters, Z , and masses, M , which are depicted in Fig. 11. The tracks extend over the MS (in some cases) and post-MS part of the pulsation instability range. The relative hydrogen abundance $X=0.72$ and the mixing length parameter $\alpha_{\text{MLT}}=1.5$ were adopted in all these models. Effects of overshooting and rotation have been ignored but this choice is not essential here.

We may see that a large range of Z -values is required to explain star positions in both diagrams. For triple-mode stars OGLE-GD-DSCT-0021 and 0034 in Table 1 we need $Z \approx 4 \times 10^{-4}$, which corresponds to Population II objects, called SX Phe stars. Similar is required for double-mode object OGLE-GD-DSCT-0032 at $\log P_F \approx -1.08$ and $P_{10}/P_F \approx 0.782$. There is one double-mode outlier, 0012, at $\log P_F \approx -0.78$ and $P_{10}/P_F \approx 0.785$, which certainly cannot be reproduced by our models. It is worth noting that β Cep stars, which are much more massive and metal rich may populate this part of the diagram. To explain positions of stars OGLE-GD-DSCT-0025, 0033, 0048, and 0049 and a number

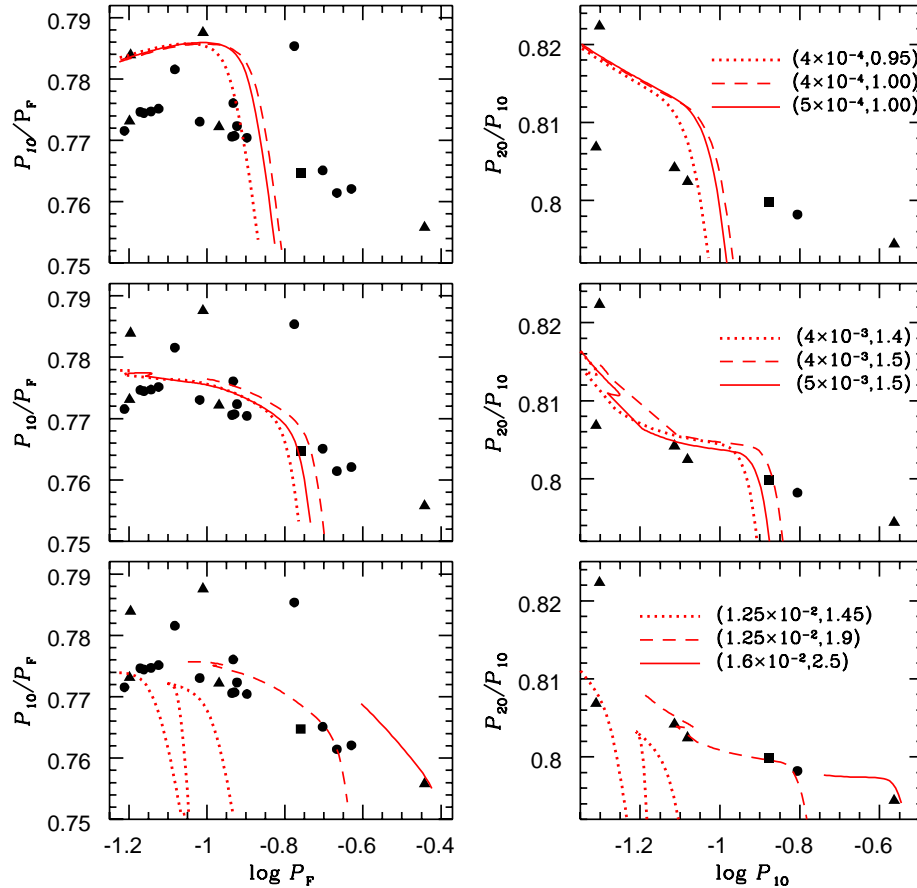


Figure 11: Location in the Petersen diagrams of objects with more than one *bona fide* radial mode detected compared with the model predictions. The left and right panels refer to the (F,1O) and (1O,2O) pairs, respectively. Circles, triangles, and squares refer to stars with two, three, and four radial modes detected, respectively. The same evolutionary models were used in both panels of each row. The numbers shown in the right panels give the metallicity Z and mass in M_{\odot} .

of double-mode objects, a close to solar metal abundance is needed.

With data on three radial mode periods (Table 1), adopting the same conditions as for calculations made for the models used in Fig. 11., we may try to determine exactly all stellar parameters. Proceeding this way, Moskalik & Dziembowski (2005) calculated their seismic models of two triple-mode Cepheids. We tried the same method and found that it had worked well for some of our stars but not all of them. The problem may be seen in the upper panels of Fig. 11. Consider for instance star OGLE-GD-DSCT-0021 ($\log P_F \approx -1.01$ and $P_{1O}/P_F \approx 0.788$). It is clear that there is no solution for M and Z , though we are close to models with lowest values (solid lines). We found the same for different choices of X , α_{MLT} , and α_{OV} parameters and at moderate rotation. The limited precision of our period calculations in some cases prohibited the use of this method. Thus, as the best models of all seven objects in Table 1 were chosen those minimizing $D \equiv \sqrt{\sum_k (\log P_k^{\text{obs}} - \log P_k^{\text{mod}})^2}$. Adding the 3O period

for the quadruple-mode star OGLE-GD-DSCT-0025 to that fit has a negligible effect on inferred parameters, resulting in the worse fit and the value of D going up from 0.002 to 0.005.

In Table 2, along with model parameters, we list the reddening, $E(V-I)$, and distance modulus $m-M$. These quantities were determined from the mean magnitudes measured in the two bands and the corresponding absolute magnitudes interpolated from the tables provided by Castelli and Kurucz (2004). The obtained distances range from 2.5 to 6.2 kpc, which places the seven variables in the foreground of stars from the Centaurus spiral arm.

Table 2: Parameters of our best models for seven δ Sct type stars with at least three radial modes

Variable	M	Z	Age	$\log T_{\text{eff}}$	$E(V-I)$	$m-M$	Remarks
OGLE-GD- -DSCT-	[M_{\odot}]		[Gyr]	[K]	[mag]	[mag]	
-0018	1.74	0.00848	1.16	3.862	0.37	13.00	post-MS
-0021	0.94	0.00046	5.68	3.825	0.65	13.66	SX Phe
-0025	1.92	0.01234	1.02	3.835	0.36	12.00	post-MS
-0033	1.45	0.01253	1.51	3.835	0.43	12.94	MS
-0034	1.01	0.00044	4.36	3.887	0.90	13.54	SX Phe
-0048	1.46	0.00713	1.83	3.842	0.53	13.95	post-MS
-0049	2.46	0.01618	0.58	3.789	0.58	13.85	post-MS

The main source of uncertainty in the numbers given in Table 2 is the lack of data on the relative hydrogen abundance and rotation rate as well as insufficient knowledge about efficiency of convective transport and overshooting. In order to assess the range of uncertainties, we carried out calculations with varying values of X , α_{MLT} , α_{OV} , and v_{rot} . In particular for star OGLE-GD-DSCT-0049, we obtained the following expressions for inferred parameters with an explicit dependence on these quantities:

$$\begin{aligned}
 M &= 2.46 - 3.33(X - 0.72) + 0.5(\alpha_{\text{MLT}} - 1.5) - 0.07\alpha_{\text{OV}} - 0.06\alpha_{\text{rot}}, \\
 Z &= 0.016 - 0.27(X - 0.72) + 0.11(\alpha_{\text{MLT}} - 1.5) - 0.0015\alpha_{\text{OV}} - 0.0006\alpha_{\text{rot}}, \\
 \text{Age} &= 0.58 - 0.4(X - 0.72) + 0.15(\alpha_{\text{MLT}} - 1.5) - 0.19\alpha_{\text{OV}} - 0.034\alpha_{\text{rot}}, \\
 E(V-I) &= 0.058 - 0.8(X - 0.72) + 0.16(\alpha_{\text{MLT}} - 1.5) - 0.19\alpha_{\text{OV}} - 0.034\alpha_{\text{rot}}, \\
 m-M &= 13.85 - 0.8(X - 0.72) + 0.23(\alpha_{\text{MLT}} - 1.5) + 0.15\alpha_{\text{OV}} - 0.060\alpha_{\text{rot}},
 \end{aligned}$$

where

$$\alpha_{\text{rot}} = \left(\frac{v_{\text{rot}}}{90 \text{ km/s}} \right)^2.$$

Searching for frequencies between 24 d^{-1} and 100 d^{-1} led us to the detection of a star with the dominant period of $0.01962154(1) \text{ d} = 28.255018(1) \text{ min}$ and an exceptionally high peak-to-peak I -band amplitude of 0.35 mag. Its light curve is presented in the last panel of Fig. 8. The object shows two additional peaks equally distant from the dominant mode in the frequency space: $\pm 1.9028 \text{ d}^{-1}$ from 50.9644 d^{-1} (Fig. 12). The high amplitude at the very short pulsation period causes a problem with proper classification of this object. It seems to be an extreme case of δ Sct type stars. In the revised catalog of 636 δ Sct stars prepared by Rodriguez *et al.* (2000), nineteen objects have periods below or

around 0.03 d, and only three objects below or around 0.02 d. The corresponding maximum V -band amplitudes are 0.06 mag and 0.02 mag, respectively. A similar triple-peak structure of the oscillation spectrum was found in the δ Sct star 1 Mon (V474 Mon): $7.3461 \pm 0.1291 \text{ d}^{-1}$. Balona and Stobie (1980) interpreted that structure as a dipolar ($\ell = 1$) triplet, where the dominant peak is due to a radial mode and the two side oscillations are likely dipole modes split by stellar rotation. If the three peaks in our star are due to a dipolar triplet then $\nu_{\text{rot}} \approx 1.9 \text{ d}^{-1}$, which implies $v_{\text{rot}} \sim 100R/R_{\odot} \approx 150 \text{ km/s}$, well acceptable value for a δ Sct type object. Therefore we named this intriguing object as OGLE-GD-DSCT-0058.

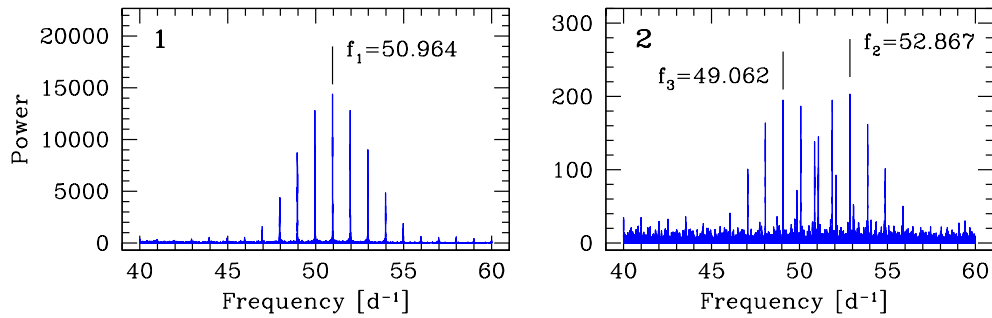


Fig. 12. Power spectra of the short-period pulsator OGLE-GD-DSCT-0058 with labelled frequencies.

4.6 Other short-period pulsators

In the observed Galactic fields, we detected 60 stars with periods $< 0.23 \text{ d}$, I -band variability range $> 0.05 \text{ mag}$, and shapes characteristic for pulsating stars. Fifty-two of the stars show more than one periodicity, but the period ratios cannot be explained by the presence of pure radial modes in δ Sct. In some of the stars we observe close, very likely non-radial modes (see Fig. 13). In Fig. 14, we present the I vs. $V - I$ diagram for one of the OGLE fields with marked locations of the short-period stars. Most of the objects are probably δ Sct type stars, but we cannot exclude that some of them are more distant β Cep type stars. Information on spectral type would help in the final classification of these objects.

4.7 Pulsating white dwarf

The high-frequency search ($24\text{--}100 \text{ d}^{-1}$) led us to the initial detection of nearly one hundred objects with a signal-to-noise ratio $S/N > 10$. All but one objects have $V - I > 0.3 \text{ mag}$. The blue outlier with $V - I \approx -0.23 \text{ mag}$ has the period of $0.01273972(1) \text{ d} = 1100.712(1) \text{ s}$ and the full I -band amplitude of 0.010 mag . The observed color, period, and amplitude are typical for pulsating white dwarfs, for instance of ZZ Cet type (*e.g.*, Eggen 1985, Van Grootel *et al.* 2012). Phased light curve of OGLE-GD-WD-0001 is shown in Fig. 15.

5 Completeness of the search

The completeness of the search for pulsating stars depends on their type. All our Classical Cepheids were detected during the inspection of stars with a signal-to-noise ratio $S/N \geq 14$. We did not find any new Cepheid among objects with

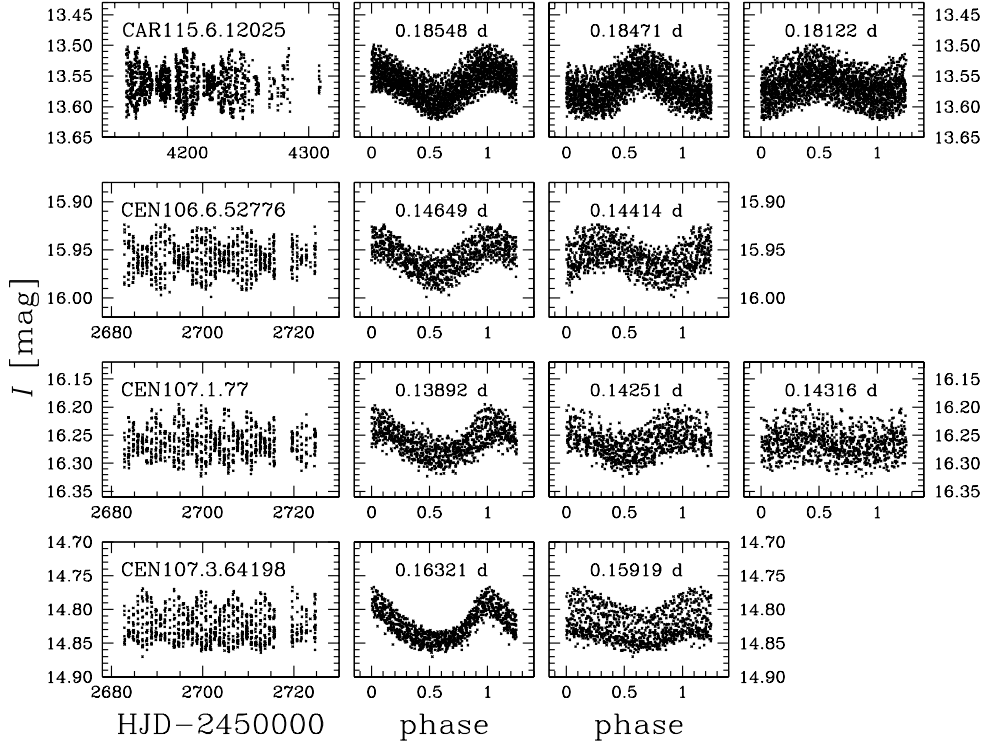


Fig. 13. Example light curves of short-period pulsators showing two or more close modes. These stars could be either δ Sct or β Cep type variables, but due to the lack of information on intrinsic color or surface temperature it is almost impossible to distinguish between the two types.

$10 \leq S/N < 14$. The discovered Cepheids are bright and have the average I -band magnitudes < 16.5 . Given the brightness and the corresponding rms variability $\sigma_I < 0.03$ mag (Szymański *et al.* 2010) it is highly unlikely we missed a single Cepheid. Therefore, we conclude that the completeness of the survey for Classical Cepheids with amplitudes > 0.1 mag reached 100%. A close to 100% completeness also holds for the RRab type stars of which only one has a $S/N < 14$. Sinusoidal-like RRc type objects are difficult to distinguish from hundreds of regularly variable candidate spotted stars and some pulsators of this type could be missed. Their completeness could be as low as 50%.

For LPVs the completeness seems to depend on the time coverage of the fields. We did not detect these variables in the fields with only one well-covered season, *i.e.*, CAR106, CEN106, and CEN107. The new LPVs were found in the disk fields which contain about 83% of all monitored stars. This percentage is a rough estimate of the completeness for high-amplitude regularly pulsating LPVs, in particular the Mira variables.

Proper classification of short-period pulsators based on the VI photometry is particularly difficult for stars in the Galactic disk fields. However, the results for the fundamental-mode HADS variables seem to be very complete, since 24 objects out of the 28 detected fundamental-mode δ Sct stars were found during the inspection of stars with the variability signal-to-noise ratio $S/N \geq 14$.

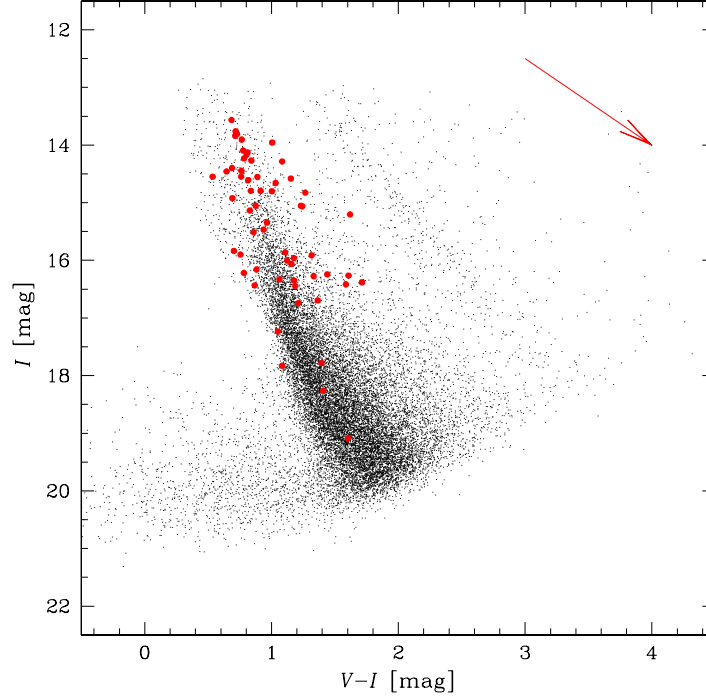


Fig. 14. Color-magnitude diagram of the field CAR113.4 located about $0^{\circ}.9$ from the Galactic plane with the location of 58 unclassified short-period pulsators (red points). Red arrow indicate the direction of reddening with an assumed ratio of total-to-selective extinction $R_I = A_I/E(V-I) = 1.5$.

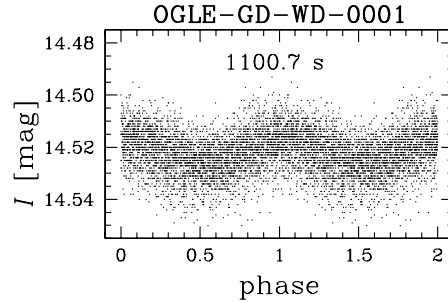


Fig. 15. Light curve of the pulsating white dwarf detected in the OGLE Galactic disk area.

6 Summary of the search for pulsating stars

Twenty-one fields in the direction tangent to the Centaurus Arm of the Galactic disk were observed by the OGLE survey during the third phase of the project in years 2001–2009. The analysis of the data has brought an identification of 20 *bona fide* Classical Cepheids, 45 RR Lyr type stars, 31 LPVs, one pulsating white dwarf, and 58 very likely δ Sct type stars. Only one of the disk variables, OGLE-GD-CEP-0019, had been identified before. Ten Cepheids are fundamental-mode, two are first-overtone, and eight are double-mode pulsators, mainly F/10 and 10/20. One Cepheid, OGLE-GD-CEP-0001, pulsates in the first overtone and a second mysterious mode. All detected Classical Cepheids

are brighter than $I = 16.4$ mag, which is about 5 mag above the survey limit. We also report six candidates for Type II Cepheids.

Among the RR Lyr variables, 36 stars are of the RRab type and nine of the RRc type. The photometrically derived metallicities for RRab variables indicate the presence of stars from two populations: metal poor stars of the Galactic halo and metal rich stars of the thick disk.

Twenty-eight of the identified δ Sct type stars pulsate in the fundamental mode. In 22 stars of this type we found two radial modes, in six stars three radial modes, and in one object four radial modes. Many stars exhibit additional non-radial modes. The presence of more than two radial modes in seven stars allowed the determination of their distance and physical parameters based on pulsation models. We show that two triple-mode and one double-mode stars are very likely Population II pulsators of SX Phe type. We note that star OGLE-GD-DSC-T-0012 cannot be reproduced by our models. It could be either a δ Sct type star pulsating in some non-radial modes or, less probable, a β Cep type star. Information on spectral type would help in the definitive classification of this and another 60 short-period pulsating variables found in the OGLE disk area. Among the detected stars there is also a candidate δ Sct star with an exceptionally high full I -band amplitude of 0.35 mag at the very short period of 0.0196 d.

The detection completeness of Classical Cepheids, RRab type stars, and fundamental-mode δ Sct type stars with amplitudes > 0.1 mag and brightness $I < 18$ mag is assessed at the level of 100%. In the case of the RRc variables several stars could be missed. The search for LPVs was estimated to be complete in about 83%.

The OGLE photometry in the disk fields allowed a confident classification of Classical Cepheids, RR Lyr, most of LPVs and some δ Sct type variables. However, many other types of pulsating variables, besides β Cep type stars, are very likely present in the data. Among them could be low-amplitude Cepheids, SPB stars, γ Dor type stars, hybrid β Cep/SPB (Pamyatnykh 1999), δ Sct/ γ Dor stars (Grigahcène *et al.* 2010), and pulsating M dwarfs (Rodríguez-López, MacDonald and Moya 2012). Similar periods, small amplitudes, and sinusoidal-like light curves of the variables make them extremely difficult to discriminate from candidate spotted stars.

7 The OGLE-IV Galactic Disk Survey

The detection of new Classical Cepheids is one of the aims of a new Galactic survey conducted in the framework of the OGLE-IV project at the 1.3-m Warsaw telescope. The survey covers more than half of the Galactic plane with longitudes from -170° to $+60^\circ$ and latitudes $-3^\circ \lesssim b \lesssim +3^\circ$. By taking 30 s exposures we plan to find variables in a brightness range $10 < I < 18$ mag. In Fig. 16, we present a color image of almost entire fourth quarter of the Galactic disk with the overlaid location of the OGLE-III and OGLE-IV fields. The total OGLE-IV disk area is about 200 times larger than the area analyzed in this paper. With this coverage we plan to achieve a nearly complete census of high-amplitude Classical Cepheids.

For the purpose of the new survey we compiled data on known Galactic Classical Cepheids from the literature. The list of confirmed Classical Cepheids from the General Catalogue of Variable Stars (GCVS, Samus *et al.* 2013) was supplemented with the OGLE-III objects (this work and Soszyński *et al.* 2011b),

revised objects from the All Sky Automated Survey (ASAS) Catalogue of Variable Stars (Pojmański 1998, 2002, 2003, Pojmański and Maciejewski 2004, 2005, Pojmański, Pilecki and Szczygiel 2005) and the International Variable Star Index[†]. We used photometric data from the Northern Sky Variability Survey (NSVS, Woźniak *et al.* 2004) and the ASAS survey to estimate the pulsation periods for some Cepheids. Based on the ASAS data (G. Pojmański, private communication) we found that object V2864 Sgr with a period of 75.8 d is a LPV star, not a Cepheid. Currently, the longest period Classical Cepheid known in our Galaxy is S Vul with $P = 68.464$ d. The compiled list of 841 Galactic Classical Cepheids is also available in the on-line OGLE archive (see links in Section 3).

Fig. 17 shows the distribution of the Galactic Classical Cepheids in the (l, b) coordinates. Approximately 85% of the stars are located within a $-5^\circ < b < +5^\circ$ stripe and $\approx 64\%$ within a $-3^\circ < b < +3^\circ$ stripe along the Galactic plane. From the distribution we can infer that obscured Milky Way plane regions in the first and fourth quarters ($-90^\circ \leq l < +90^\circ$) may hide many (probably at least several hundreds) not yet detected Cepheids.

In Fig.18, we present the histogram of the pulsation periods of known fundamental-mode Galactic Classical Cepheids and compare it with period distributions for stars in the SMC (Soszyński *et al.* 2010) and LMC (Soszyński *et al.* 2008, Ulaczyk *et al.* 2013). The distribution for the Galactic Cepheids peaks at ≈ 5.0 d, while for LMC and SMC at ≈ 3.0 d and ≈ 1.5 d, respectively. This shift is a result of different metallicities and chemical evolution between the Galaxy, LMC, and SMC. A future more complete list of Galactic Classical Cepheids from OGLE-IV will be used to trace the spiral structure and star formation history of the Milky Way.

Acknowledgments. The authors would like to thank Richard I. Anderson for discussions on the presented project, Grzegorz Pojmański for his help in close inspection of selected ASAS objects, and Thomas Fruth for providing the BEST-II survey photometric data on candidates for Galactic Cepheids. This work has been supported by the Polish Ministry of Sciences and Higher Education grants No. IP2012 005672 under the Iuventus Plus program and No. IdP2012 000162 under the Ideas Plus program. W.D. is supported by the Polish National Science Centre through grant No. DEC-2012/05/B/ST9/03932. The OGLE project has received funding from the European Research Council under the European Community's Seventh Framework Programme (FP7/2007-2013)/ERC grant agreement No. 246678 to A.U.

REFERENCES

- Akhter, S., Da Costa, G. S., Keller, S. C., and Schmidt, B. P. 2012, *Astrophys. J.*, **756**, 23.
 Alard, C., and Lupton, R. H. 1998, *Astrophys. J.*, **503**, 325.
 Balona, L. A., and Stobie, R. S. 1980, *MNRAS*, **190**, 931.
 Balona, L. A., and Dziembowski, W. A. 2011, *MNRAS*, **417**, 591.
 Balona, L. A., *et al.* 2012, *MNRAS*, **419**, 3028.
 Bernhard, K., and Wils, P. 2009, *Peremennye Zvezdy Prilozhenie*, **9**, 5.
 Błażko, S. 1907, *Astron. Nachr.*, **175**, 327.
 Bobylev, V. V., and Bajkova, A. T. 2012, *Astronomy Letters*, **38**, 638.
 Bono, G., Marconi, M., Cassisi, S., Caputo, F., Gieren, W., and Pietrzyński, G. 2005, *Astrophys. J.*, **621**, 966.
 Breger, M., *et al.* 2011, *MNRAS*, **414**, 1721.
 Buchler, J. R., and Szabó, R. 2007, *Astrophys. J.*, **660**, 723.

[†]<http://www.aavso.org/vsx/>

- Buchler, J. R. 2008, *Astrophys. J.*, **680**, 1412.
- Castelli, F., and Kurucz R. L. 2004, , astro-ph/0405087.
- Daszyńska-Daszkiewicz, J., Dziembowski, W. A., and Pamyatnykh, A. A. 2005, *Astron. Astrophys.*, **441**, 641.
- Derue, F., *et al.* 2002, *Astron. Astrophys.*, **389**, 149.
- Eggen, O. J. 1985, *P.A.S.P.*, **97**, 1029.
- Freedman, W. L. *et al.* 1994, *Astrophys. J.*, **427**, 628.
- Genovali, K., *et al.* 2013, *Astron. Astrophys.*, **554**, A132.
- Gieren, W., Pietrzyński, G., Walker, A., Bresolin, F., Minniti, D., Kudritzki, R.-P., Udalski, A., Soszyński, I., Fouqué, P., Storm, J., and Bono, G. 2004, *Astron. J.*, **128**, 1167.
- Gieren, W., *et al.* 2013, *Astrophys. J.*, **773**, 69.
- Greco, C., Clementini, G., Catelan, M., Held, E. V., Poretti, E., Gullieuszik, M., Maio, M., Rest, A., DeLee, N., Smith, H. A., and Pritzl, B. J. 2009, *Astrophys. J.*, **701**, 1323.
- Grigahcène, A. *et al.* 2010, *Astrophys. J.*, **713**, L192.
- Jurcsik, J. 1995, *Acta Astron.*, **45**, 653.
- Kanbur, S. M., Ngeow, C.-C., and Buchler, J. R. 2004, *MNRAS*, **354**, 212.
- Kanbur, S. M., Marconi, M., Ngeow, C., Musella, I., Turner, M., James, A., Magin, S., and Halsey, J. 2010, *MNRAS*, **408**, 695.
- Kinemuchi, K., Smith, H. A., Woźniak, P. R., and McKay, T. A. 2006, *Astron. J.*, **132**, 1202.
- Kinman, T. D., Morrison, H. L., and Brown, W. R. 2009, *Astron. J.*, **137**, 3198.
- Lee, Y.-H., Kim, S. S., Shin, J., Lee, J., and Jin, H. 2008, *PASJ*, **60**, 551.
- Lemasle, B. *et al.* . 2013, *Astron. Astrophys.*, **558**, A31.
- Li, Z. P., Xu, Y., and Li, Q. S. 2010, *P.A.S.P.*, **122**, 1432.
- Luck, R. E., Andrievsky, S. M., Kovtyukh, V. V., Gieren, W., and Graczyk, D. 2011, *Astron. J.*, **142**, 51.
- Majaess, D. J., Turner, D. G., and Lane, D. J. 2009, *MNRAS*, **398**, 263.
- Mateu, C., Vivas, A. K., Downes, J. J., Briceño, C., Zinn, R., and Cruz-Díaz, G. 2012, *MNRAS*, **427**, 3374.
- Menzies, J. W., Whitelock, P. A., Feast, M. W., and Matsunaga, N. 2010, *MNRAS*, **406**, 86.
- Miceli, A., Rest, A., Stubbs, C. W., Hawley, S. L., Cook, K. H., Magnier, E. A., Krisciunas, K., Howell, E., and Koehn, B. 2008, *Astrophys. J.*, **678**, 865.
- Moskalik, P., and Dziembowski, W.A. 2005, *Astron. Astrophys.*, **434**, 1077.
- Mróz, P., Pietrukowicz, P., Soszyński, I., Udalski, A., Poleski, R., Szymański, M. K., Kubiak, M., Pietrzyński, G., Wyrzykowski, L., Ulaczyk, K., Kozłowski, S., and Skowron, J. 2013, *Acta Astron.*, **63**, 135.
- Neilson, H. R., Langer, N., Engle, S. G., Guinan, E., and Izzard, R. 2012, *Astrophys. J.*, **760**, L18.
- Pamyatnykh, A. A. 1999, *Acta Astron.*, **49**, 119.
- Paparo, M., *et al.* 2013, *Astron. Astrophys.*, **557**, A27.
- Pietrukowicz, P. 2003, *Acta Astron.*, **53**, 63.
- Pietrukowicz, P., Udalski, A., Soszyński, I., Nataf, D. M., Wyrzykowski, L., Poleski, R., Kozłowski, S., Szymański, M. K., Kubiak, M., Pietrzyński, G., and Ulaczyk, K. 2012, *Astrophys. J.*, **750**, 169.
- Pietrukowicz, P., Mróz, P., Soszyński, I., Udalski, A., Poleski, R., Szymański, M. K., Kubiak, M., Pietrzyński, G., Wyrzykowski, L., Ulaczyk, K., Kozłowski, S., and Skowron, J. 2013, *Acta Astron.*, **63**, 115.
- Pietrzyński, G., Gieren, W., Szewczyk, O., Walker, A., Rizzi, L., Bresolin, F., Kudritzki, R.-P., Nalewajko, K., Storm, J., Dall'Ora, M., and Ivanov, V. 2008, *Astron. J.*, **135**, 1993.
- Pojmański, G. 1998, *Acta Astron.*, **48**, 35.
- Pojmański, G. 2002, *Acta Astron.*, **52**, 397.
- Pojmański, G. 2003, *Acta Astron.*, **53**, 341.
- Pojmański, G. and Maciejewski, G. 2004, *Acta Astron.*, **54**, 153.
- Pojmański, G. and Maciejewski, G. 2005, *Acta Astron.*, **55**, 97.
- Pojmański, G., Pilecki, B., and Szczygiel, D. M. 2005, *Acta Astron.*, **55**, 275.
- Poleski, R. 2008, *Acta Astron.*, **58**, 313.
- Poleski, R., Soszyński, I., Udalski, A., Szymański, M. K., Kubiak, M., Pietrzyński, G., Wyrzykowski, L., Szewczyk, O., and Ulaczyk, K. 2010, *Acta Astron.*, **60**, 1.
- Popielski, B. L., Dziembowski, W. A., and Cassisi, S. 2000, *Acta Astron.*, **50**, 491.
- Popova, M. É. 2006, *Astronomy Letters*, **32**, 244.
- Rejkuba, M. 2004, *Astron. Astrophys.*, **413**, 903.
- Riess, A. G., Fliri, J., and Valls-Gabaud, D. 2012, *Astrophys. J.*, **745**, 156.
- Rodríguez, E., López-González, M. J., and López de Coca, P. 2000, *Astron. Astrophys. Suppl. Ser.*, **144**, 469.
- Rodríguez-López, C., MacDonald, J., and Moya, A. 2012, *MNRAS*, **419**, L44.
- Samus, N. N., *et al.* 2013, , General Catalog of Variable Stars, Version: Apr 2013.

- Sarajedini, A., Mancone, C. L., Lauer, T. R., Dressler, A., Freedman, W., Trager, S. C., Grillmair, C., and Mighell, K. J. 2009, *Astron. J.*, **138**, 184.
- Schwarzenberg-Czerny, A. 1996, *Astrophys. J.*, **460**, L107.
- Sesar, B., *et al.* 2010, *Astrophys. J.*, **708**, 717.
- Smith, H. A. 2004, *Camb. Astrophys. Ser.*, **27**, “RR Lyrae Stars”, Cambridge University Press.
- Smolec, R. 2005, *Acta Astron.*, **55**, 59.
- Soszyński, I., Poleski, R., Udalski, A., Szymański, M. K., Kubiak, M., Pietrzyński, G., Wyrzykowski, L., Szewczyk, O., and Ulaczyk, K. 2008, *Acta Astron.*, **58**, 163.
- Soszyński, I., Poleski, R., Udalski, A., Szymański, M. K., Kubiak, M., Pietrzyński, G., Wyrzykowski, L., Szewczyk, O., and Ulaczyk, K. 2010, *Acta Astron.*, **60**, 17.
- Soszyński, I., Dziembowski, W. A., Udalski, A., Poleski, R., Szymański, M. K., Kubiak, M., Pietrzyński, G., Wyrzykowski, L., Ulaczyk, K., Kozłowski, S., and Pietrukowicz, P. 2011a, *Acta Astron.*, **61**, 1.
- Soszyński, I., Udalski, A., Pietrukowicz, P., Szymański, M. K., Kubiak, M., Pietrzyński, G., Wyrzykowski, L., Ulaczyk, K., Poleski, R., and Kozłowski, S. 2011b, *Acta Astron.*, **61**, 285.
- Soszyński, I., Udalski, A., Szymański, M. K., Kubiak, M., Pietrzyński, G., Wyrzykowski, L., Ulaczyk, K., Poleski, R., Kozłowski, S., Pietrukowicz, P., and Skowron, J. 2013, *Acta Astron.*, **63**, 21.
- Stankov, A., and Handler, G. 2005, *Astrophys. J. Suppl. Ser.*, **158**, 193.
- Storm, J., Gieren, W., Fouqué, P., Barnes, T. G., Soszyński, I., Pietrzyński, G., Nardetto, N., and Quéloz, D. 2011, *Astron. Astrophys.*, **534A**, 95.
- Suárez, J. C., Andrade, L., Goupil, M. J., and Janot-Pacheco, E. 2010, *Astron. Nachr.*, **331**, 1073.
- Süveges, M. *et al.* 2012, *MNRAS*, **424**, 2528.
- Szczygieł, D. M., Pojmański, G., and Pilecki, B. 2009, *Acta Astron.*, **59**, 137.
- Szymański, M. K., Udalski, A., Soszyński, I., Kubiak, M., Pietrzyński, G., Poleski, R., Wyrzykowski, L., and Ulaczyk, K. 2010, *Acta Astron.*, **60**, 295.
- Szymański, M. K., Udalski, A., Soszyński, I., Kubiak, M., Pietrzyński, G., Poleski, R., Wyrzykowski, L., and Ulaczyk, K. 2011, *Acta Astron.*, **61**, 83.
- Tammann, G. A., Reindl, B., and Sandage, A. 2011, *Astron. Astrophys.*, **531**, A134.
- Turner, D. G., Abdel-Sabour Abdel-Latif, M., and Berdnikov, L. N. 2006, *P.A.S.P.*, **118**, 410.
- Udalski, A., Szymański, M., Kaluzny, J., Kubiak, M., and Mateo, M. 1992, *Acta Astron.*, **42**, 253.
- Udalski, A. 2003, *Acta Astron.*, **53**, 291.
- Udalski, A., Szymański, M. K., Soszyński, I., and Poleski, R. 2008, *Acta Astron.*, **58**, 69.
- Ulaczyk, K., Szymański, M. K., Udalski, A., Kubiak, M., Pietrzyński, G., Soszyński, I., Wyrzykowski, L., Poleski, R., Gieren, W., Walker, A. R., and Garcá-Varela, A. 2013, *Acta Astron.*, **63**, 159.
- Van Grootel, V., Dupret, M.-A., Fontaine, G., Brassard, P., Grigahcène, A., and Quirion, P.-O. 2012, *Astron. Astrophys.*, **539**, A87.
- Vilardell, F., Jordi, C., and Ribas, I. 2007, *Astron. Astrophys.*, **473**, 847.
- Whitelock, P. A., Menzies, J. W., Feast, M. W., Matsunaga, N., Tanabé, T., and Ita, Y. 2009, *MNRAS*, **394**, 795.
- Woźniak, P. R. 2000, *Acta Astron.*, **50**, 421.
- Woźniak, P. R., *et al.* 2004, *Astron. J.*, **127**, 2436.
- Yang, S.-C., Sarajedini, A., Holtzman, J. A., and Garnett, D. R. 2010, *Astrophys. J.*, **724**, 799.

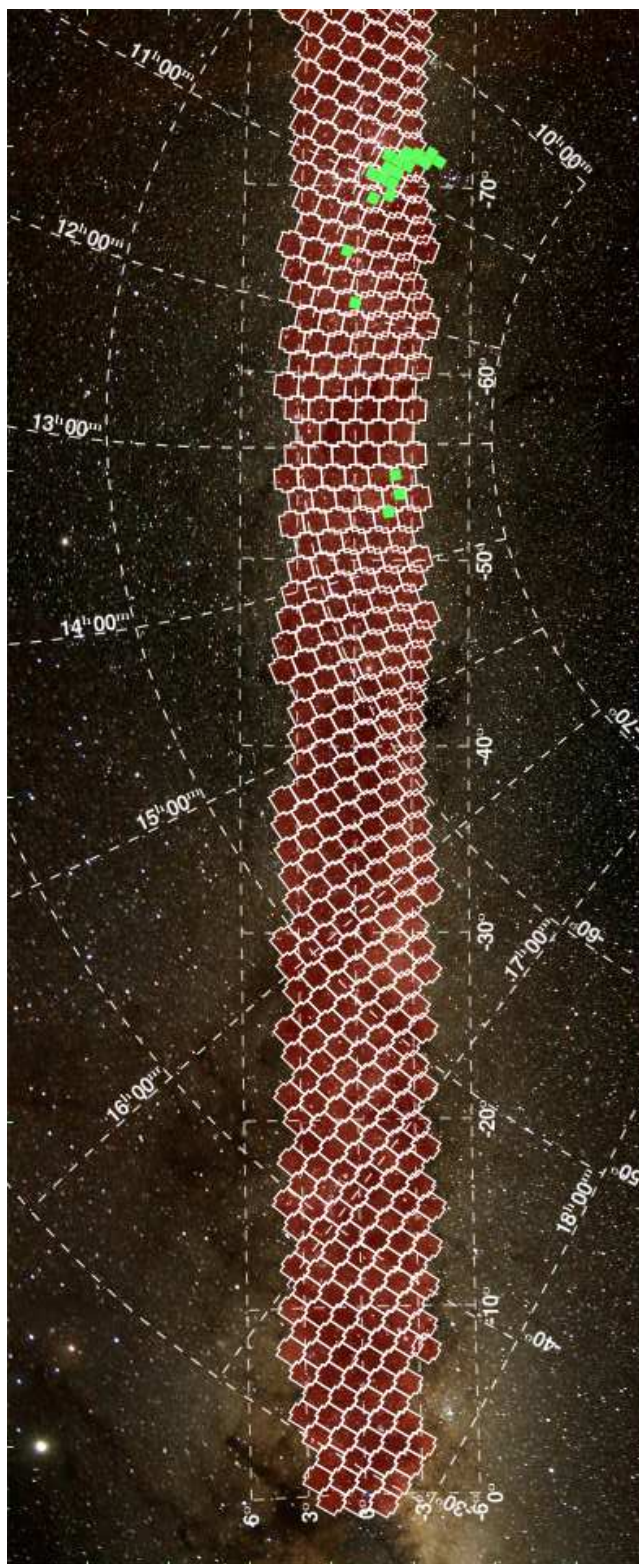


Fig. 16. Map of the OGLE-IV Galactic Disk Survey fields with longitudes between -80° and 0° . Dashed white lines mark the equatorial and Galactic coordinate grids. The whole OGLE-IV disk survey covers the Galactic plane between longitudes $-170^\circ \lesssim l \lesssim +60^\circ$ and latitudes $-3^\circ \lesssim b \lesssim +3^\circ$. Green filled squares denote the location of the OGLE-III fields analyzed in this paper.

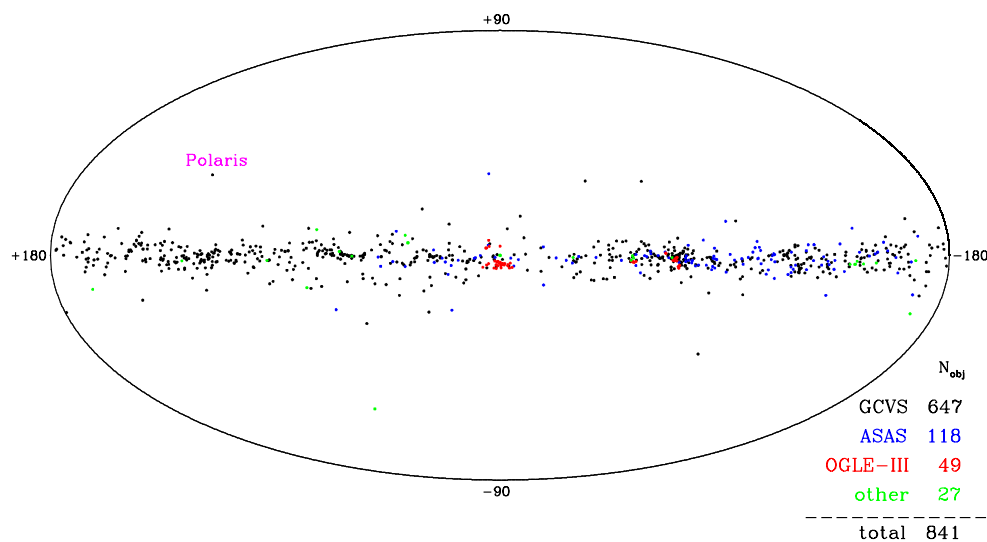


Fig. 17. Distribution of the Milky Way's Classical Cepheids in Galactic coordinates in equal area Mollweide's projection.

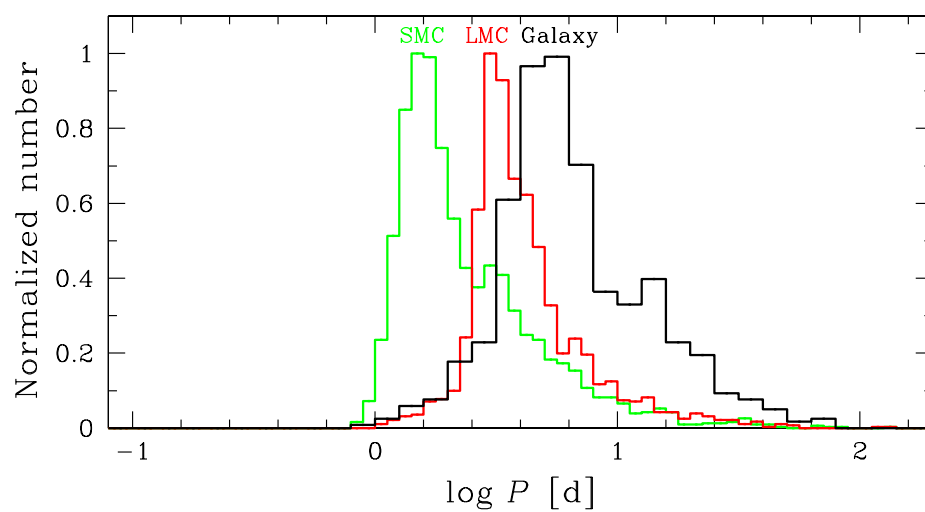


Fig. 18. Comparison of the period distributions for fundamental-mode Classical Cepheids in the SMC, LMC, and our Galaxy (2626, 1851, and 664 objects, respectively).

